



# Skeletal anomalies in gilthead seabream (*Sparus aurata*) larvae reared in different densities and water volumes

Zachary Dellacqua<sup>1,2</sup>  | Claudia Di Biagio<sup>1,3</sup> | Arianna Martini<sup>4,5</sup>  |  
 Francesco Mattei<sup>4,6</sup> | Arnold Rakaj<sup>4</sup> | James C. Williams Jr.<sup>7</sup> |  
 Andrea Fabris<sup>8</sup> | Marisol Izquierdo<sup>2</sup> | Clara Boglione<sup>4</sup>

<sup>1</sup>PhD Program in Evolutionary Biology and Ecology, University of Rome 'Tor Vergata', Rome, Italy

<sup>2</sup>Grupo de Investigación en Acuicultura (GIA), Ecoaqua Institute, University of Las Palmas de Gran Canaria, Las Palmas de Gran Canaria, Spain

<sup>3</sup>Laboratory of Evolutionary Developmental Biology, University of Ghent, Ghent, Belgium

<sup>4</sup>Department of Biology, University of Rome 'Tor Vergata', Rome, Italy

<sup>5</sup>CREA—Consiglio per la ricerca in agricoltura e l'analisi dell'economia agraria (CREA)—Centro di ricerca Zootecnia e Acquacoltura, Monterotondo, Italy

<sup>6</sup>UMR 7093, Laboratoire d'Océanographie de Villefranche (LOV), Sorbonne University, Villefranche-sur-mer, France

<sup>7</sup>Department of Anatomy, Cell Biology and Physiology, Indiana University School of Medicine, Indianapolis, Indiana, USA

<sup>8</sup>Associazione Piscicoltori Italiani, Verona, Italy

## Correspondence

Zachary Dellacqua, PhD Program in Evolutionary Biology and Ecology, University of Rome 'Tor Vergata', Rome 00133, Italy.  
 Email: [dellacquaz95@gmail.com](mailto:dellacquaz95@gmail.com)

## Funding information

European Union's Horizon 2020 research and innovation program 'BIOMEDAQU', Grant/Award Number: 766347

## Abstract

This study describes the effects on the skeletal phenotype of two pivotal factors, density and water volume, on the hatchery (larval) phase of gilthead seabream (*Sparus aurata*) larvae previously described for two model species (*Danio rerio* and *Oryzias latipes*) and sub-adult (pre-ongrowing) gilthead seabream (*Sparus aurata*). The experimental trial was conducted using single conditions in a pilot study, starting with a total of 615,385 eggs from the same batch. Three densities (LD low density: 25 larvae/L; MD medium density: 125 larvae/L; and HD high density: 250 larvae/L) and two water volumes (500 and 1000 L) were tested from spawning

This is an open access article under the terms of the [Creative Commons Attribution-NonCommercial-NoDerivs](https://creativecommons.org/licenses/by-nc-nd/4.0/) License, which permits use and distribution in any medium, provided the original work is properly cited, the use is non-commercial and no modifications or adaptations are made.

© 2024 The Authors. *Journal of the World Aquaculture Society* published by Wiley Periodicals LLC on behalf of World Aquaculture Society.

up to 60 days post-hatching (dph) (average standard length: 1.79 cm; average dry weight: 27.11 mg). On the final samples, morphometric, anatomical, and histological data were collected for data pertinent to meristic counts and skeletal anomalies. The results (analyzed by means of multivariate analyses) indicated that the LD-reared larvae were significantly longer and heavier than HD-reared fish. Furthermore, LD-reared gilthead seabream exhibited a significant reduction in the frequency of individuals with anomalies of jaws, vertebral body shape, and vertebral arches than the MD and HD conditions, which is in agreement with previous experiments carried out on model species and gilthead seabream sub-adults.

#### KEYWORDS

hatchery phase, larval rearing, skeletal anomalies, *Sparus aurata*, stocking density, water volume

## 1 | INTRODUCTION

The production of gilthead seabream (*Sparus aurata*) and European seabass (*Dicentrarchus labrax*) together make up the second most important aquaculture industry in the European Union (*European Parliament Fact Sheet*, 2018). However, recent data from 2017 and 2018 have revealed increased production while the profitability has declined as a result of high production costs and oversupply (Llorente et al., 2020). Therefore, a focus on increasing the products' value rather than increasing production quantity could offer a sustainable solution to improve profitability and adjust for long-term environmental and economic goals in the EU.

One of the limiting factors reducing the farms' profitability is consumer skepticism towards aquaculture products, since aquaculture products sometimes present different appearances than wild-caught fish, especially when intensively reared. In the case of gilthead seabream, darker pigmentation, a roundish body profile, and externally detectable skeletal anomalies are the main features that enable the distinguishing between reared and wild fish (Boglione, Gisbert, et al., 2013). Furthermore, the presence of skeletal anomalies negatively impacts the well-being of the fish, as deformed fish can be more susceptible to parasites (i.e., when opercular reductions are present) or feed less effectively (if affected by severe anomalies in the jaws or vertebral column). The zootechnical approaches aimed at increasing production quantity have led researchers to investigate the effects of genetic variability and fitness, inbreeding, selective breeding of desired quantitative traits (Afonso et al., 2000; Berillis, 2017; Fragkoulis et al., 2018, 2020), proper nutritional requirements (Baeverfjord et al., 2019; Cahu et al., 2003; Darias et al., 2011; Dominguez et al., 2021, 2022; Ferosekhan et al., 2022; Georga et al., 2011; Izquierdo et al., 2017, 2019; Lall & Lewis-McCrea, 2007; Sivagurunathan et al., 2022; Tseng et al., 2021); and the use of superficial skimmers (Chatain & Ounais-Guschemann, 1990), on growth and skeletal quality (viz. targeting to reduce the incidence of skeletal anomalies). Despite the many studies elucidating factors that elicit skeletal anomalies the problem has persisted and many challenges still remain evident (Boglione, Gavaia, et al., 2013; Eissa et al., 2021; Kourkouta et al., 2022). This is in part a result of the complex etiology of skeletal anomalies: different causative factors can induce the same skeletal anomaly in different species; different environmental factors often act synergistically and can either have a negative impact (worsening the deformation) or a positive impact (recovery of a deformation) (Fragkoulis et al., 2019; Witten et al., 2006), depending on the species and/or the life stage.

Taking into consideration that it is still under debate if marine farmed fish can be considered 'domesticated' animals (as in the terrestrial zootechnical species), an 'ecological' approach has been applied by some scientific studies that have compared the effects on skeletal anomalies of semi-intensive (mesocosms (Divanach & Kentouri, 2000) or large volume conditions (Cataudella et al., 2003): volumes of 40–60 m<sup>3</sup> coupled with densities of 3–16 larvae/L; Prestinicola et al., 2013) versus intensive rearing conditions (volumes of 0.5–9 m<sup>3</sup> coupled with densities of ~100 larvae/L), demonstrating that semi-intensive strategies yield fish with fewer skeletal anomalies in marine fish, such as dusky grouper, *Epinephelus marginatus* (Boglione et al., 2009), and in gilthead seabream larvae and juveniles (Boglione et al., 2001; Prestinicola et al., 2013). Nevertheless, intensive farmers still look for cost-effective options to reduce the incidences of skeletal anomalies without having to incorporate the larger and more costly tanks. Similarly, in more recent studies, the separated effects of low densities versus water volumes were investigated in certain fish models. For example, the experimental rearing of zebrafish (*Danio rerio*), from 30 to 90 dpf (days post fecundation), at three different densities (high density HD: 32 fish/L; medium density MD: 8 fish/L; low density LD: 2 fish/L) showed that the rearing density significantly influenced the specimens' average standard length (SL) (lower SL with increasing rearing density). Further, the HD lot showed the highest number of deformities per specimen, the highest number of observed types of deformities and, together with the MD group, the highest frequency of specimens affected by severe deformities. In particular, these deformities affected the arches, spines, and vertebral centra in the hemal region of the vertebral column (Martini et al., 2021). A further study, carried out on zebrafish from the same life-stage and reared at 8 individuals/L in 3 L (MD, small volume), 20 individuals/L in 3 L (HD, small volume), and 20 individuals/L in 12 L (HD, large volume) showed that the lowest tested density (MD) yielded significantly longer zebrafish. Furthermore, density resulted to be the main driver affecting the skeleton, as increasing the water volumes did not mitigate the negative effects of HD: the frequency (%) of anomalies and individuals grouped by skeletal region or region/element did not reveal any clear trend linking space availability and skeletal phenotypes from this particular study (Di Biagio, 2022). Another recent work on medaka (*Oryzias latipes*) reared from 0 to 40 dph (days post hatching) at three different densities (LD: 5 individuals/L, MD: 15 individuals/L, and HD: 45 individuals/L) demonstrated that LD produced significantly longer juveniles and reduced incidences of anomalies affecting the preural vertebral centra, and the caudal fin endoskeleton and dermal rays (Di Biagio et al., 2022). Additionally, a follow-up study on the effects of tank volume in mitigating the development of skeletal anomalies in medaka, testing a density of 40 fish/L in 3 versus 6 L tanks, confirmed the results found in zebrafish with another model fish species: that increased swimming space did not mitigate the negative effects of HD on the skeleton of medaka (Di Biagio, 2022). Concerning reared commercial species, a similar approach has been applied to gilthead seabream (*Sparus aurata*) sub-adults (Dellacqua et al., 2023). In that work, sub-adults obtained from different spawns which had been previously selected for the absence of externally detectable skeletal anomalies, were reared from 6.7 g up to 54.9 g at 3 different densities (LD: 5, MD: 10, and HD: 20 kg/m<sup>3</sup>) in both 500 and 1000-L water volumes, for ~63 days. The results demonstrated that the gilthead seabream reared in LD were significantly longer and had significantly lower incidences of opercular and vertebral column deviations (mainly lordosis affecting the hemal vertebrae) than the HD-reared individuals. In this species, at the sub-adult life stage, the use of larger water volumes only somewhat mitigated the incidences of jaw anomalies, although not significantly.

As a result of high levels of mortality and undesirable fry quality, the hatchery phase (rearing from eggs to juveniles) remains to be a predominant bottleneck in marine fish culture (Hamre et al., 2013). The morphological quality of juveniles is crucial for obtaining a satisfactory quantity of final marketable product. Even though skeletal anomalies can arise up until harvest at market size, most skeletal anomalies develop in the early life stages.

In this scenario, this study aims at verifying if the same positive effects of low rearing density and mitigating effects of greater available water volume on the development of skeletal anomalies are detectable in gilthead seabream reared during the hatchery (larval rearing) phase from eggs up to 60 dph, in two different water volumes (1000 vs. 500 L), and stocked at three different initial densities. This approach foresaw: (i) that the tested densities were those considered of interest to fish farmers (Italian Fish Farmers Association (API)); (ii) that the water volumes were identical to those previously used in the experimental rearing during the pre-ongrowing phase in the same

species (Dellacqua et al., 2023) and were significantly larger than tanks or aquaria often used for experimental studies on model fish (1–3 L Di Biagio et al., 2022; Martini et al., 2021), and commercial species like gilthead seabream (170–200 L Dominguez et al., 2021; Dominguez et al., 2022; Izquierdo et al., 2017; Izquierdo et al., 2019; Sivagurunathan et al., 2022; Tseng et al., 2021). Furthermore, these large tanks required a very large number of fish (initial number of eggs = 615,385) to be subjected to the experimental trial.

## 2 | MATERIALS AND METHODS

### 2.1 | Ethics statement

Animal experiments were conducted in compliance with the European Union Directive (2010/63/EU) and Spanish legislation (Royal Decree 53/2013) for the protection of animals for scientific purposes at the ECOAQUA Institute, University of Las Palmas of Gran Canaria (ULPGC, Canary Islands, Spain). All experiments conducted at ULPGC were approved by the Bioethical Committee of the ULPGC (REF: 007/2012 CEBA ULPGC).

### 2.2 | Experimental rearing

The experiment was carried out in 2019 from mid-April to mid-June with gilthead seabream (*Sparus aurata*) reared from eggs up to an early juvenile stage (60 days post-hatching, hereafter denoted dph). Eggs were obtained from natural spawns of the gilthead seabream broodstock from the Grupo de Investigación en Acuicultura (GIA) (Table S1) at the ECOAQUA Institute. Eggs were collected and incubated overnight, held in a 315-micron mesh net in an incubating tank with a renovation of 25% seawater/h. Eggs were then transferred into the experimental tanks and overstocked with respect to the average hatching rate from the broodstock group used (~97.5%), in order to have the following initial densities: Low Density (LD, 25 larvae/L); Medium Density (MD, 125 larvae/L); High Density (HD, 250 larvae/L). All density conditions were tested in cylindrical fiberglass tanks, 3 containing 1000 L (1 m<sup>3</sup>) and 3 containing 500 L (0.5 m<sup>3</sup>) of water. The resulting six experimental conditions are hereafter referred to as LD1000, MD1000, HD1000, LD500, MD500, and HD500.

Subsets of eggs ( $n = 192$ ), from the same spawning, were maintained in two 96-well plates in an incubating chamber (at a temperature of 20°C and natural photoperiod, as was carried out for the experimental fish) in order to calculate the spawning quality, the fertilization, hatching rates, and the effective survival rate at 3 dph (calculated according to the method described by Ferosekhan et al., 2020).

The tanks were supplied with continuous running seawater which passed through a UV and sand filtration system then entered the tanks via a flow-through system starting from the center of the tank basin and exited through a 500- $\mu$ m mesh-covered outlet filter. Daily maintenance included manual surface skimming, siphoning the tank bottom, and cleaning the mesh outlet covers. The photoperiod was based on natural light during the spring-time months of April to June in the Canary Islands (ranging from 12–14 h/day throughout the rearing period). Natural seawater was filtered and pumped into the system at a steady rate of 15% per hour until the eggs had hatched; it was then reduced to 5% per hour up to the first feeding upon depletion of the yolk sac, and slowly increased up to 25% replacement per hour (which equated to 4.16 L/min in the 1000-L conditions and 2.08 L/min in the 500-L conditions). Every morning at 8 a.m., 1 L of cultured phytoplankton (*Nannochloropsis* sp., containing 3–4  $\times 10^7$  cells/mL) was poured directly into the inlet of each tank for every 100 L of water volume. The phytoplankton was cultured in 50-L bags with an initial inoculation density of 5  $\times 10^6$  cells/mL at a salinity of 25 ppt and regular ambient temperatures during this rearing season in the Canary Islands. Phytoplankton cell densities were calculated by placing mixed samples from the 50-L bag on a microscope slide with a grid and visually counting cells within each grid section. Enriched (Origreen and Orione, Skretting) rotifers (*Brachionus plicatilis*) were added to the tanks and the

concentrations were checked several times throughout the day by taking water samples to determine the present rotifer density which was adjusted to maintain a density of 10 individuals/mL by adding rotifers when necessary. Upon the gilthead seabream larvae reaching an average size of 4.5 mm (14 dph), enriched (Origreen and Orione, Skretting) *Artemia salina* nauplii and metanauplii were added to the tank twice per day in a quantity sufficient to maintain a density of 0.5 individuals/mL of seawater, up to 31 dph, and then augmented to 1 individual/mL of seawater. Starting at 25 dph, fish began to be weaned with Gemma microdiet dry feeds of 75, 150, 300, and 500 microns consecutively (Skretting, Norway) and fed ad libitum hourly during the daylight hours. Throughout experimental rearing tanks had an average water temperature of  $22.4 \pm 1.0^\circ\text{C}$  (Figure S1a). The average dissolved oxygen ( $5.4 \pm 0.6$  mg/L) was monitored hourly and regulated in order to maintain a saturation level above  $70.0 \pm 7.3\%$  (Figure S1b). All of the experimental tanks were manually skimmed throughout the day to eliminate surface oil, allowing larvae to properly access the surface for proper swim bladder inflation. After the effective survival rate at 3 dph was checked on the subset of larvae from the same spawn, the estimated densities in the tanks at the beginning of the experiment resulted to be slightly lower (22, 116, and 209 larvae/L) than the desired ones (25, 125 and 250 larvae/L). Nevertheless, this affected the fish in all the conditions proportionately, thus maintaining the differences between the LD, MD, and HD lots.

The experimental rearing ended when seabream reached 60 dph (SL >16 mm), at the early juvenile stage (Faustino & Power, 1998).

## 2.3 | Sampling

At the end of the experimental rearing (60 dph), the juveniles were euthanized with an overdose of clove oil (1 mL/L of seawater); 100 individuals/condition were photographed and measured for length and weight; another set of 300 individuals/condition were fixed (1.5% paraformaldehyde PFA, 1.5% glutaraldehyde in 0.1 M sodium cacodylate buffer, pH 7.4), then dehydrated after 24 h following a series of graded ethanol and stored in 70% ethanol for subsequent anatomical analyses.

## 2.4 | Post-rearing measurements

The final survival was calculated with respect to the number of larvae in each tank at the beginning of the trial on the basis of the survival rate estimated at 3 dph on the subset of eggs. Then at the end of the experimental rearing, all the juveniles were individually counted in each tank to calculate the final survival. Daily mortality could not be monitored as a result of the use of the green water technique which makes the tank water eutrophic and dead larvae were not identifiable.

Total length (TL) and SL measurements were obtained using a ruler and a profile projector (Mitutoyo PJ-3000A, Kanagawa, Japan).

Weight measurements were taken by pre-weighing blank slides, then placing 4 gilthead seabream individuals per slide which were weighed immediately for the wet weights (WW). The slides (with the gilthead seabream) were then dried in the oven and weighed again to calculate the dry weight (DW) (COBOS precision scale, Barcelona, Spain).

### 2.4.1 | Anatomical analyses

A total of 949 juveniles (60 dph) were whole-mount stained with Alizarin red S following a modified protocol (Taylor & Van Dyke, 1985). Mass monitoring of meristic counts, skeletal anomalies, and swim bladder inflation was conducted using an AxioZoom V.16 (Zeiss) stereomicroscope. Data on skeletal anomalies were recorded following an adapted alphanumeric code (Prestinicola et al., 2013) (Table S2). The analyses were carried out based on the

following assumptions: (1) incomplete fused bone elements were counted separately as discrete elements (i.e., a fusion of 2 rays that were still discernibly separate at some location along the ray were considered for meristic counts as 2 rays); (2) supernumerary bones (additional bones) with normal morphology were not considered to be anomalies but were included in the meristic count; conversely, anomalous supernumerary elements were included among anomalies; (3) only clearly and unquestionably identifiable variations in shape were considered as skeletal anomalies. Skeletal anomaly data were expressed in a raw matrix (RM) and used to calculate the frequencies (%) of each type of anomaly over the total number of anomalies in each group. The RM was subsequently transformed into a binary matrix (BM) which was used to calculate the prevalence (%) of individuals affected by each anomaly type. The following metrics were calculated for each experimental lot: (1) relative frequency (%) of individuals with at least one anomaly; (2) number of anomaly types observed; (3) malformation index (number of total anomalies/number of malformed individuals); (4) relative frequency (%) of individuals with at least one severe anomaly (anomalies affecting the head, the vertebral axis, or vertebral centra); (5) relative frequency (%) of observed severe anomalies over the total number of observed anomalies; (6) severe anomalies' load (number of severe anomalies/number of individuals with severe anomalies); (7) frequency (%) of each anomaly type over the total number of anomalies.

## 2.5 | Ordination models and statistical analyses

A Correspondence Analysis (CA; Benzecri, 1975) was performed on an RM constituted of grouped anomalies (grouped RM) according to the body region and the skeletal type (listed in Table S3). A Principal Component Analysis (PCA) was applied to performance data and some grouped skeletal anomalies (listed in Table S3), selected on the basis of the presence of significant differences in occurrence among the six conditions. The differences in the occurrence of grouped anomalies (listed in Table S3) among the rearing conditions were statistically tested using a general  $\chi^2$  test and  $\chi^2$  pairwise post-hoc tests (Pearson, 1900); which were chosen based on different groupings of biological significance (i.e., externally detectable, severe, and affecting a high frequency of individuals) from the BM. The False Discovery Rate (FDR) correction was used for multiple comparisons (Benjamini & Hochberg, 1995).

Final lengths and weights were first measured for normal distribution and then subsequently tested for differences with a Kruskal-Wallis and Dunn's post-hoc with Bonferroni correction.

Statistical analyses and graphs were carried out using Python 3.8.0 (Van Rossum & Drake Jr, 1995).

## 2.6 | MicroCT and histology

Seventy fixed samples were scanned using a Micro CT Skyscan 1172 (Bruker) at the Indiana University School of Medicine (scan parameters included a 60 kVp x-ray source with a 0.5 mm Al filter, and a final image voxel size of 6–10  $\mu\text{m}$ ) and reconstructed using the software AMIRA (Thermo Fisher Scientific). Four of the scanned samples were selected for subsequent histological analyses and after rehydration from ethanol, were decalcified for 4 weeks by submersion in 10% EDTA, 0.5% PFA at 4°C and then embedded in GMA (glycol methacrylate) resin (Witten et al., 2001). Sections (5  $\mu\text{m}$ ) were cut on a standard rotary microtome (Microm HM360, Marshall Scientific) and stained with toluidine blue.

# 3 | RESULTS

## 3.1 | Post-harvest data

The final survival was greatest and statistically different from all the other conditions in the LD500 condition ( $\chi^2$  pairwise post hoc with Bonferroni correction,  $p < 0.05$ ), with a 29.7% survival of early juveniles at 60 dph. The

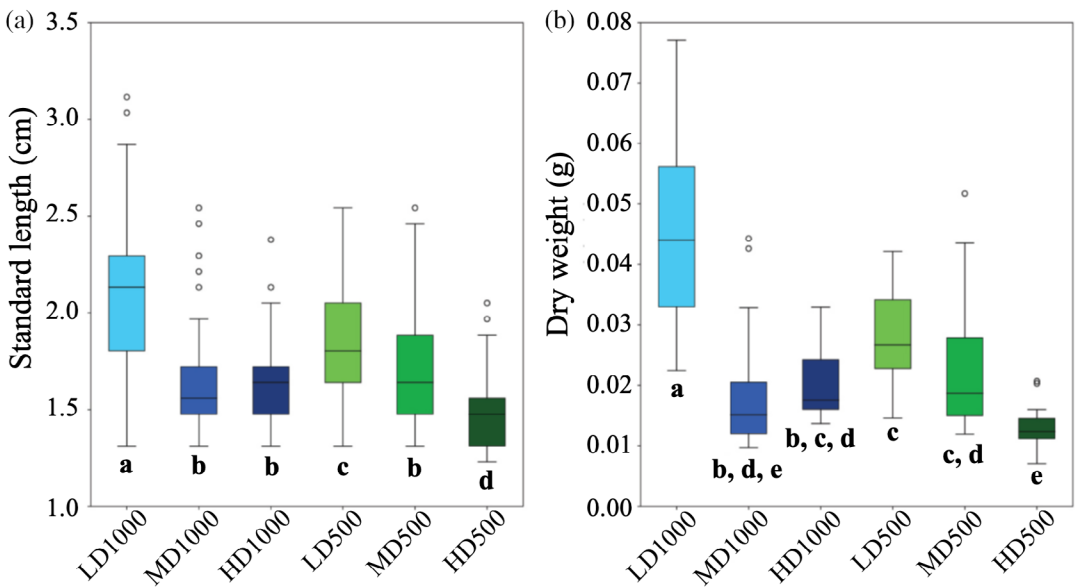


**FIGURE 1** (a) Box & whisker plots of SL (cm) and (b) DW(g) of gilthead seabream individuals (100 individuals/condition) sampled after 60dph. Box indicates the central percentile, the line inside the box is the median while the whiskers represent the minimum and maximum values. Different letters below each box and whisker indicate statistically significant differences between conditions: therefore, conditions that are significantly different do not share any of the same letters ( $p < 0.05$ , Kruskal-Wallis, Dunn's post hoc with Bonferroni correction).

LD1000 condition had the second-highest final survival of 10%. The other conditions showed lower survival, with the lowest found to be 3.3% in the HD1000 (Table S4).

Final TL, SL, WW, and DW were found not to be normally distributed ( $p < 0.01$ , Shapiro-Wilk) and resulted to be significantly different among the conditions ( $p < 0.05$ , Kruskal-Wallis). In particular, the LD1000 rearing condition produced both the longest and the heaviest gilthead seabream juveniles, followed by the LD500 condition, while the HD500 condition produced the smallest and most lightweight seabream. The other three conditions (MD1000, HD1000, MD500), however, were not significantly different from each other (Figure 1;  $p < 0.05$ , Kruskal-Wallis, Dunn's post hoc with Bonferroni correction).

## 3.2 | Anatomical analyses

### 3.2.1 | Meristic counts

The meristic counts from the experimental lots did not differ greatly from the variations observed in wild gilthead seabream (Table S5).

Regarding the vertebral body count, a maximum of 26 vertebrae (instead of 25, as found in wild lots) was found in the MD500 lot and a minimum of 23 (instead of 24 vertebrae) was found in LD500, LD1000, and HD1000. However, recovered (an advanced stage of vertebrae fusion, in which the fused vertebral bodies are reshaped to assume the typical amphicoelic aspect; see Figure 3a) vertebral fusions, identifiable by a longer vertebral body, were present in three out of the seven juveniles with 23 vertebrae.



### 3.2.2 | Skeletal anomalies

The frequencies (%) of each anomaly type over the total number of the anomalies detected within the group and the frequencies (%) of individuals affected by each anomaly type are given, for each experimental lot, in Tables S6a and S6b. The descriptive metrics of skeletal anomalies are given in Table 1. Nearly all of the examined gilthead seabream individuals had at least one anomaly. There were no individuals found with uninflated swim bladders.

As many as 70 different anomaly types were observed, with a maximum of 64 in a single lot (HD500). Both LD1000 and LD500 had the lowest malformation index (7) and frequencies of individuals with severe anomalies (28% and 40% respectively), while the MD1000 and HD500 lots showed the highest malformation index (18) (Table 1). The highest frequencies of individuals with severe anomalies were found in both HD1000 (56%) and HD500 (52%). The HD500 lot also revealed the greatest range of anomaly types (64). The observed severe anomalies affecting the vertebral column and centra were fusions (Figure 2a), partial fusions (Figure 2b), hemivertebrae (Figure 2c), and localized scoliosis (Figure 2d). In the head (Figure 3), other severe anomalies were found to affect the maxillary, premaxillary (Figure 3b), dentary (Figure 3c,e), and the opercular plates (Figure 3d,f). The following sections report detailed descriptions of the observed anomalies.

### 3.2.3 | Head anomalies

In the HD1000 condition, 57% of the individuals were affected by cranial (neuro- and splanchnocranium) anomalies, while the LD1000 seabream displayed the lowest prevalence (28%) of affected specimens (data not shown). In both the 1000-L and the 500-L conditions, the incidence of seabream exhibiting cranial anomalies increased as the respective stocking density increased (LD < MD < HD; Figure 4). The prevalence of cranial anomalies among the 500-L conditions ranged approximately from 40% to 52% respectively from LD to HD, while the 1000-L conditions had a wider range of disparity between the density groups, ranging approximately from 28% to 57% prevalence among individuals from LD to HD (data not shown). When considering jaw anomalies, a similar trend was exhibited, with an increasing prevalence in affected individuals as the density increases (Figure 4a). Pughead (Figure 3b) and underbite (Figure 3c) were the most frequent of these splanchnocranium anomalies for which the lowest prevalence was found in LD1000 (15%) while the highest was in HD500 (35%) (Figure 4a). Often, they occurred in association with mesethmoid (neurocranium) anomalies (i.e., pughead). A relationship between increased frequencies of jaw anomalies and augmentation of density is easily discernible, however, there was also a 'volume effect' which is evidenced by the higher prevalence of jaw anomalies found in the 500-L volumes. The occurrence of individuals with jaw anomalies was lower in the 1000-L than in the 500-L tanks for each tested density. In particular, 15% of individuals in the LD1000 condition had jaw anomalies versus 22% found in the LD500, 27% in MD1000 versus 30% in MD500, and 30% in HD1000 versus 35% in HD500. Opercular plate anomalies were the least prevalent head anomaly in each condition (with frequencies of affected individuals ranging from 2.0% to 9.2%), although they still

**TABLE 1** Descriptive skeletal metrics among the experimental lots.

	LD1000	MD1000	HD1000	LD500	MD500	HD500
Number of individuals	197	149	152	149	152	150
Frequency (%) of malformed individuals	98	99	98	96	98	<b>100</b>
Malformation index	7	<b>18</b>	12	7	14	<b>18</b>
Observed anomaly types	53	55	49	52	56	<b>64</b>
Frequency (%) of individuals with severe anomalies	28	42	<b>56</b>	40	49	52



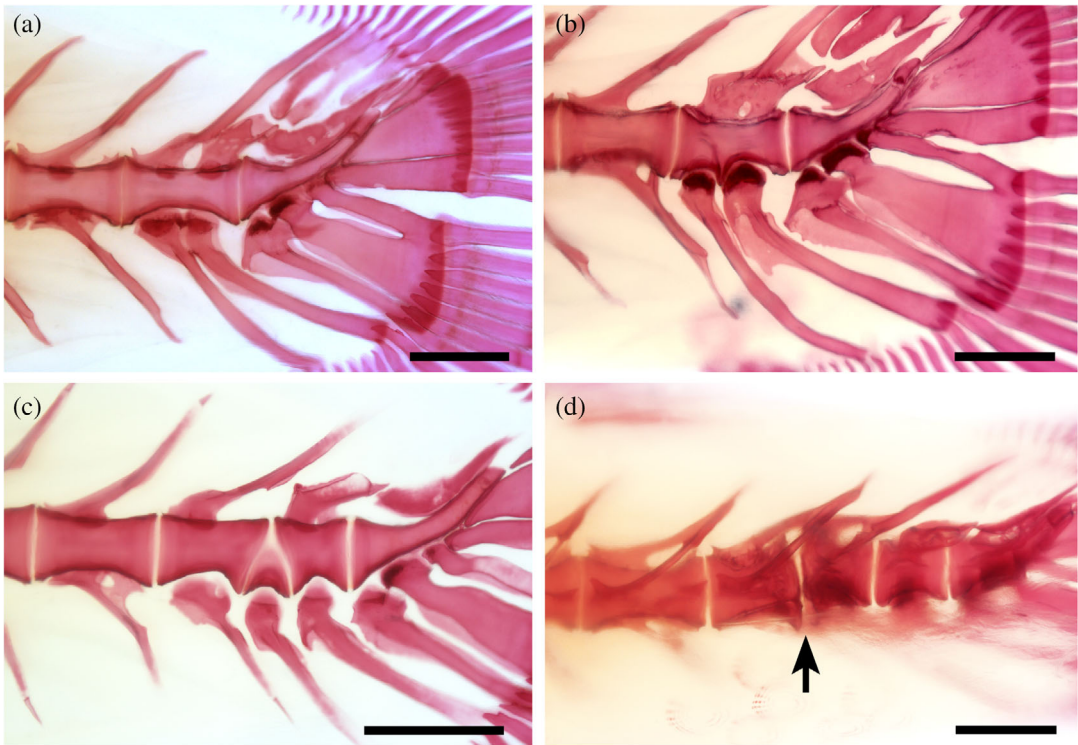


**FIGURE 2** (a) Lateral perspective of a caudal vertebra displaying a recovery from a previous fusion of the centra. Note the elongated vertebral body (arrow), the two neural elements, and the two hemal arches that are already fused proximally, and diverging distally. (b) Lateral perspective of a caudal vertebra displaying an intermediate step in the recovery process from a fusion (arrow). The dorsal region has a remodeled lining and one modified neural arch (created from the fusion between the neural arch of preural vertebrae PU3 and the spur of PU2). In the ventral region, the two fused centra are still detectable in the lining, each with their respective hemal arch. (c) Lateral perspective of a ventrally located hemivertebra (dashed rectangle), which maintained its hemal but not the neural arch. (d) Dorsal perspective displaying two vertebrae (arrow) that deviated from the longitudinal orientation of the axis, resulting in a localized lateral displacement (scoliosis) of the vertebral centra that appeared deformed. Compared with the normal vertebral body (asterisk) preceding the two-scoliotic vertebral centra. Scale bars = 0.5 mm.

exhibited an increasing rate of incidence from LD to HD (Figure 3b). Contrary to jaw anomalies, lower incidences of opercular plate anomalies were found in 500-L tanks than in 1000-L tanks for both the MD and HD density lots (for MD and HD: 500 L < 1000 L), and no difference in frequency was found between the LD500 and the LD1000 condition (LD500 = LD1000, ~2%).

### 3.2.4 | Anomalies affecting the vertebral column and associated elements

The anomalies of the vertebral axis that were considered in this study were kyphosis, lordosis, and scoliosis. Although neither kyphosis nor lordosis were found, a few of the specimens exhibited scoliosis (Figure 5). In general, the most frequently affected regions of the vertebral column were the abdominal and hemal regions (see Prestinicola et al., 2013 for the description of body regions), in which fish with anomalous centra and associated elements were found in all conditions indiscriminately (Figure 6). In particular, the vertebral arches and spines resulted to be more

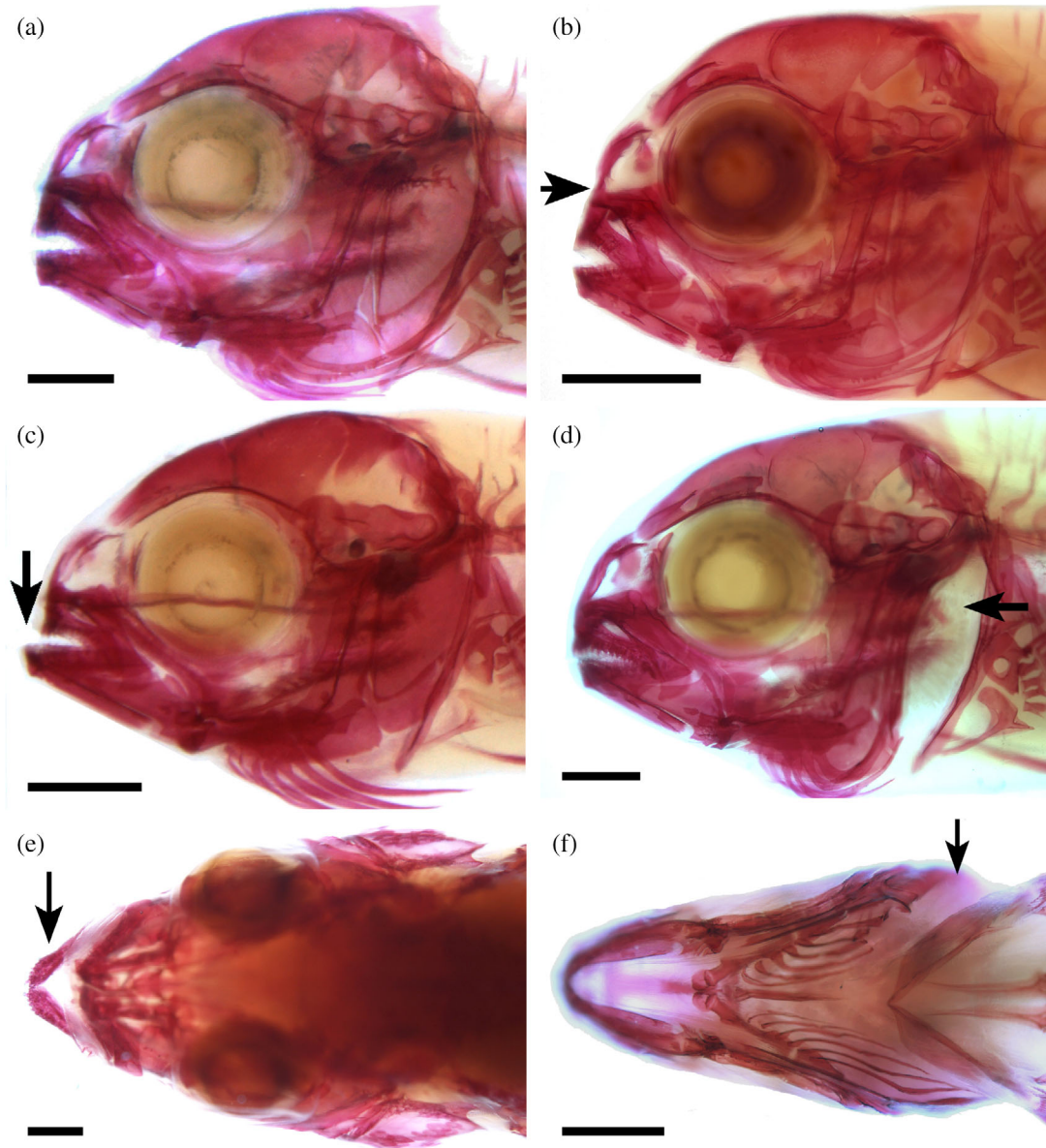


**FIGURE 3** (a) Gilthead seabream specimen with a normal cranium. (b) Specimen exhibiting a light pughead, characterized by a compressed snout (arrow). (c) Lateral (top) and (e) dorsal view (bottom) of a specimen exhibiting an underbite, characterized by a protruding dentary. (d) Lateral (top) and (f) ventral view (bottom) of a specimen with folded left opercular plate (arrow). Scale bars = 1 mm.

affected by anomalies than the corresponding centra, in each region (Figure 6). Individuals affected by anomalous neural arches in the caudal region (anomaly type D5\*) were much more common than hemal ones (D6\*), although this trend is reversed for the hemal region in which hemal arches (C6\*) were more frequently deformed than neural arches (C5\*) (Figure 7). Some examples of anomalies that were found in the elements attached to the centra are reported in Figures 8 and 9. In general, the incidence of arch anomalies was often higher in the MD and HD conditions than in the LD conditions (Figure 7), and no clear 'volume effect' could be detected. The frequencies of

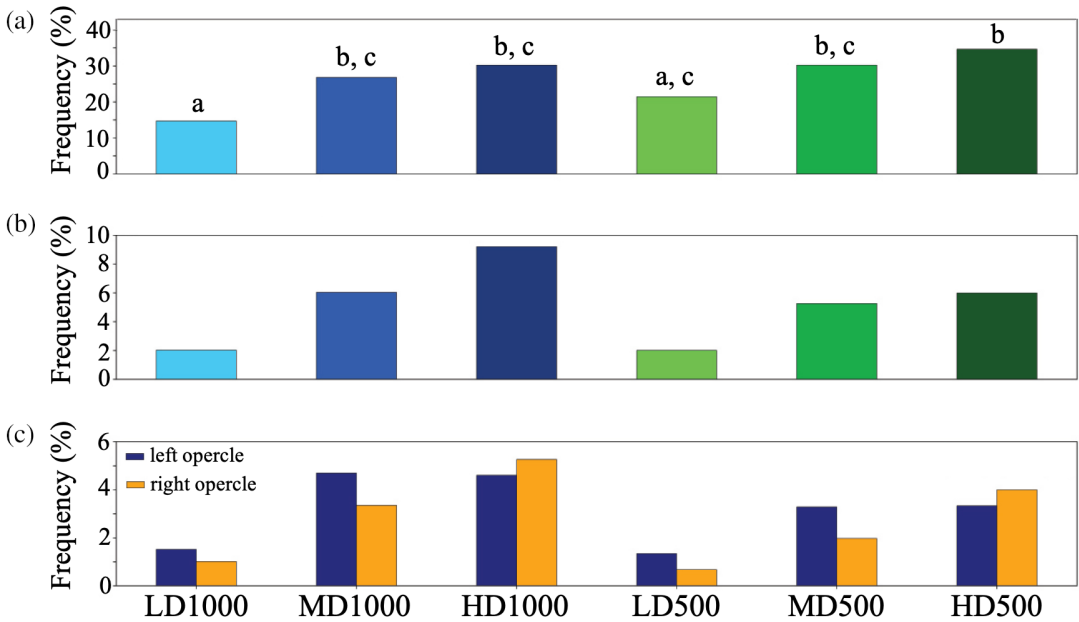


**FIGURE 4** Frequency (%) of individuals affected by (a) jaw (pre-maxillary, maxillary, and dentary) anomalies; (b) opercular anomalies of at least one-side; (c) anomalies of the left or right opercular plate, in each experimental lot. Different letters above each histogram in (a) indicate statistically significant differences between conditions: therefore, conditions which are significantly different do not share any of the same letters ( $p < 0.05$ ,  $\chi^2$  pairwise post hoc with Bonferroni correction). In (b) and (c) there were no significant pairwise differences between the conditions, although the general  $\chi^2$  for opercular anomalies resulted to be significantly different among the conditions ( $p < 0.05$ ).

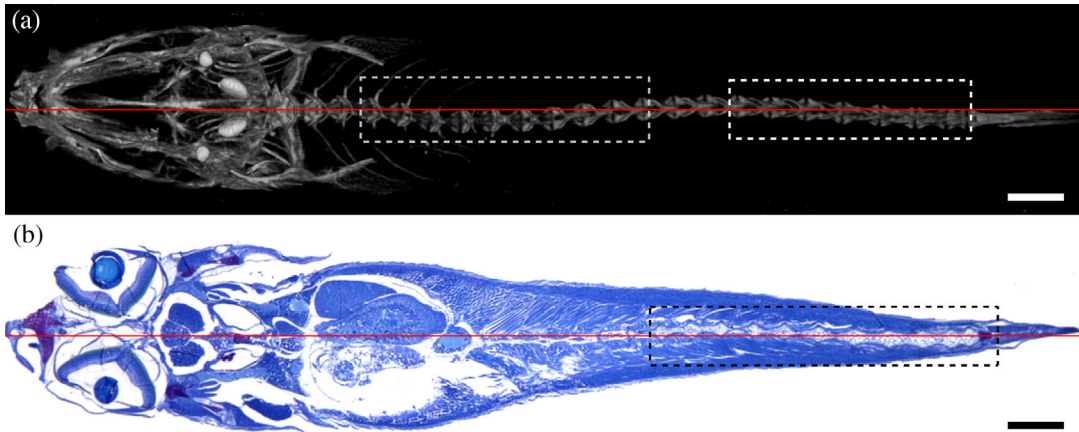


**FIGURE 5** (a) Micro-CT reconstruction (dorsal view) of a gilthead seabream juvenile (SL = 17.79 mm) exhibiting scoliosis starting in the abdominal region. The dashed rectangles delimit the scoliotic vertebrae deviating on the left (gray rectangle) and on the right and left (white rectangle) from the central vertebral axis (red line) (b) Tangential section of the same fish, note the difference in the distances between the vertebral bodies and the right and left body edge (vertebrae delimited by the black rectangle), which is a distinctive feature of scoliosis. Toluidine blue staining. Scale bars = 1 mm.

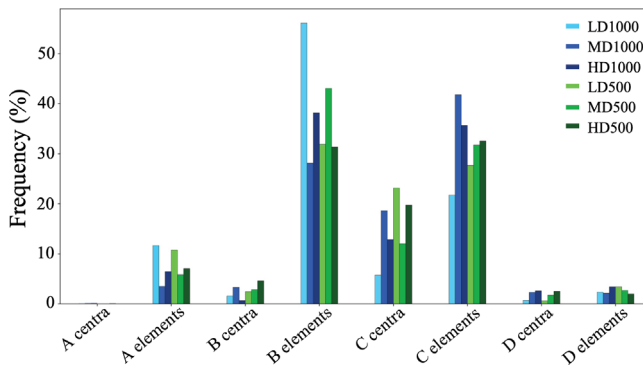


**FIGURE 6** Relative frequency (%) of anomalies affecting the vertebrae in different regions of the vertebral column (A = cephalic region, B = abdominal region, C = hemal region, and D = caudal region) from gilthead seabream reared in each of the experimental conditions. The category ‘elements’ includes the neural and hemal arches, the ribs, and the spur.

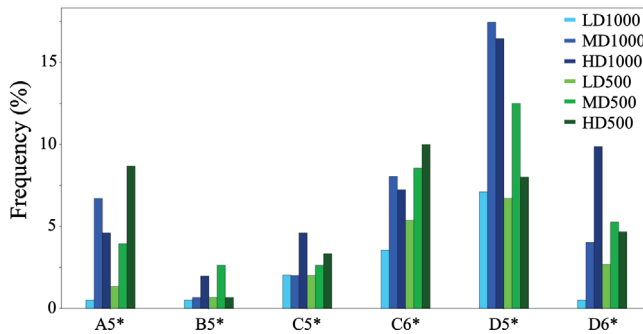


**FIGURE 7** Frequency (%) of individuals affected by anomalous arches and spines (5\* & 6\*), in each experimental condition. A5\* = supernumerary or absence of neural element in the cephalic vertebrae region. B5\* = supernumerary or absence of neural element in the abdominal vertebrae region. C5\* = supernumerary or absence of neural element in the hemal vertebrae region. C6\* = supernumerary or absence of hemal element in the hemal vertebrae region. D5\* = supernumerary or absence of neural element in the caudal vertebrae region. D6\* = supernumerary or absence of hemal element in the caudal vertebrae region. There were no significant differences between pairwise conditions.

individuals with severe vertebral anomaly types (viz. scoliosis, centra fusion, and hemivertebrae) demonstrated the presence of a clear density effect, with more affected fish in the higher density conditions (Figure 10a), following the same trend described for the anomalies of the splanchnocranium. The HD lots showed the greatest incidences (~7.2% for both HD1000 and HD500) while the lowest incidences were found in the LD conditions (~0.7% for LD500 and ~1.0% for LD1000; Figure 10a).

The incidence of severe vertebrae anomalies was primarily concentrated in the caudal region, in which completely or partially fused centra and hemivertebrae anomalies were observed (Figure S2), particularly in the HD500 and HD1000 gilthead seabream (Figure 10b). In this case, alongside a primary density effect, a secondary volume effect is discernible, with a higher prevalence in the larger volume conditions (LD1000 > LD500, MD1000 > MD500, HD1000 > HD500; Figure 10b).

The histological section and wholemount stained gilthead seabream showed that in the fused vertebrae, the fusion is completed dorsally, however, the two fusing centra are still distinguishable on the ventral side of the



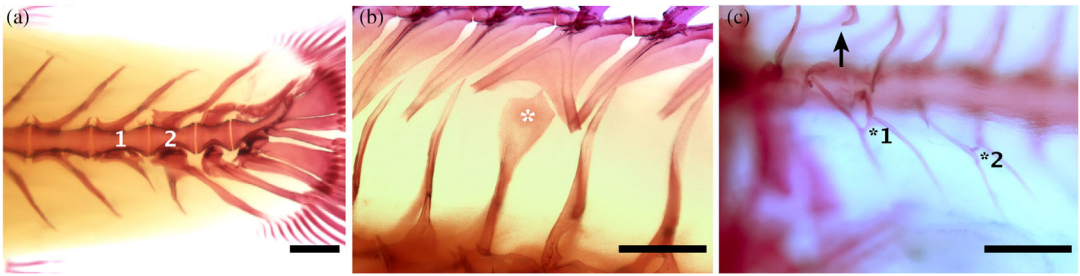


**FIGURE 8** Examples of deformed vertebra-associated elements. (a) the terminal hemal vertebra (1) shows a hemal arch that has lost the spine, which appears to be fused to the hemal arch of the following posterior vertebra (2, first caudal vertebra). (b) Flag-shaped neural spine (asterisk). Note that the above dorsal bifurcated pterygophore seemingly adapted to host the space occupied by the anomalous flag-shaped spine. (c) An abdominal vertebra (arrow) showing a missing segment of the left side of the arch (arrow), and two sets of ribs fused with each other (black asterisks 1 and 2). Note that normal arches are displayed in the preceding centra for images (a) and (b). Scale bars = 0.5 mm.

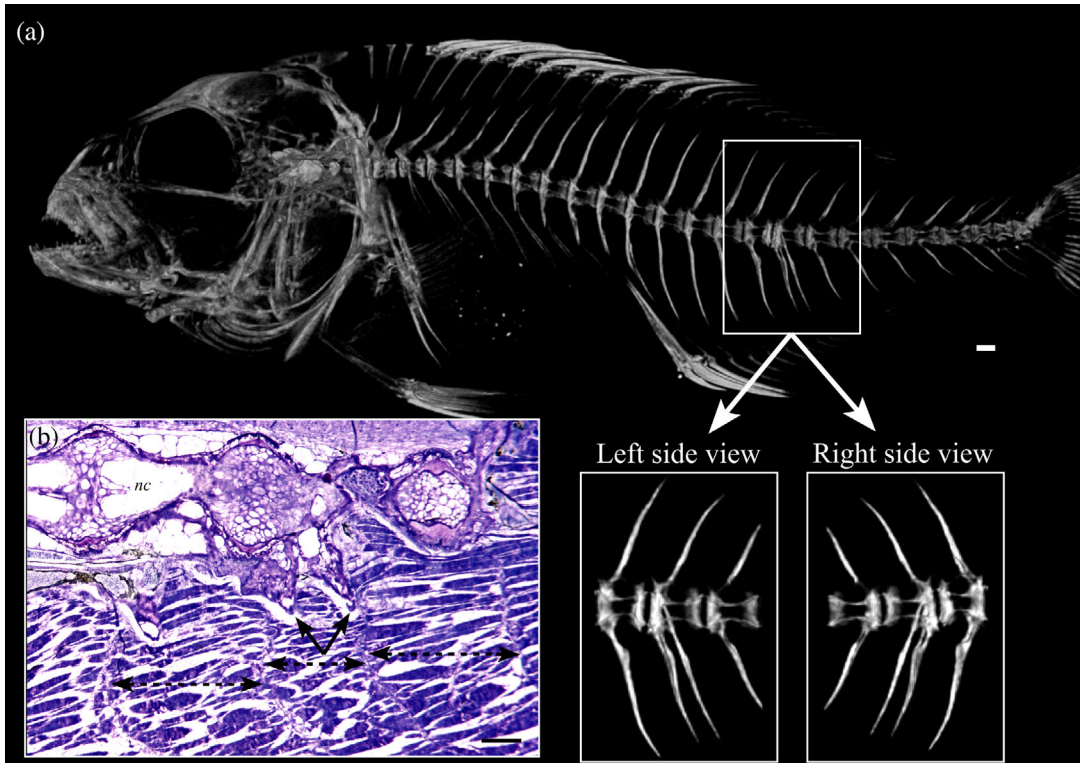


**FIGURE 9** (a) Micro-CT reconstruction of a gilthead seabream specimen (lateral view, SL = 28.0 mm) with a duplicated hemal arch element (6\*). Note that the duplication is present only on the right lateral plane of the hemal vertebral body. (b) Parasagittal section of the vertebrae highlighted in (a). Note that this and the preceding centrum are both deformed. Solid black arrows indicate the normal (on the left) and the extranumerary hemal arch element (on the right). Dashed two-way arrows indicate the myosepta delimiting myomeres, whose width changes according to the position of the arches. nc indicates the notochord. Scale bars = 0.5 mm.

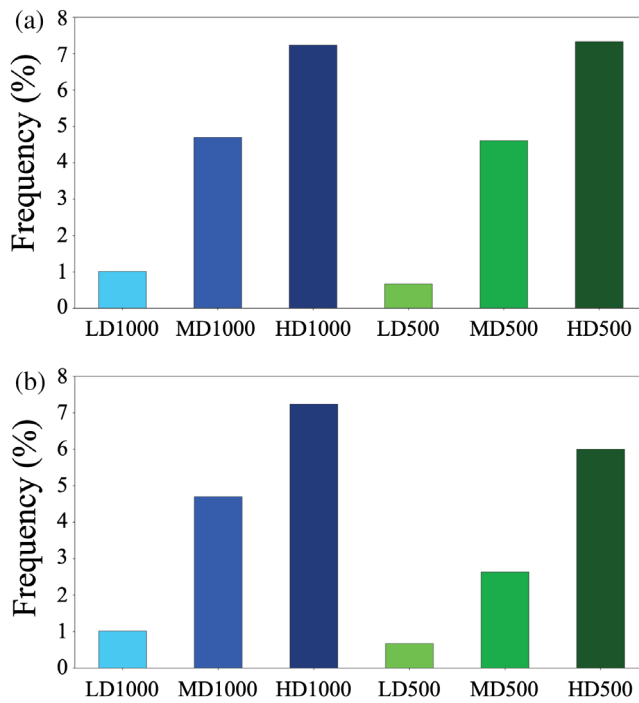


**FIGURE 10** (a) Frequency (%) of individuals affected by at least one severe vertebral anomaly (viz. scoliosis, complete and partial fusions of the centra, and hemivertebrae), in each experimental lot; (b) Frequency (%) of individuals exhibiting severe anomalies of the caudal vertebrae, in each lot. There were no significant differences between pairwise conditions.

vertebra (Figure 11c). Additionally, the presence of hyaline-rich cartilage of the neural and hemal arches is discernable both dorsally and ventrally to the fused vertebra, indicating the persistence of the two neural and two hemal arches not yet completely fused (Figure 11c).

### 3.3 | Statistical tests and ordination models

#### 3.3.1 | General $\chi^2$ and $\chi^2$ pairwise post hoc tests

In order to test the independent distribution of statistical differences in the frequencies of grouped skeletal anomalies between the rearing conditions, a general  $\chi^2$  test was performed, using six categories of anomalies. These categories were made by grouping the different types of anomalies in six groups (anomalies of the vertebral body shape, arches, opercula, jaws, vertebrae fusions, and the sum of severe head and vertebral anomalies) (Table S3). The  $p$ -values obtained with the  $\chi^2$  test are listed in Table S7, displaying that five out of these six categories resulted in significant differences ( $p < 0.05$ ) among the experimental lots, in particular, severe anomalies, arch anomalies, and vertebral body shape anomalies displayed highly significant differences ( $p$ -values  $< 0.0001$ ). Only the vertebral fusions did not show a significant difference in the pairwise comparisons, likely as a result of their low occurrences. Consequently, the  $\chi^2$  pairwise post hoc tests were carried out on the five categories that had significant differences in the general  $\chi^2$  (Table S7). The opercular anomalies group was the only one of the five anomalies categories that resulted to not have significant differences in the  $\chi^2$  pairwise post hoc. The LD1000 group was significantly different with respect to all other conditions (with the only exception of LD500 in 3 of the cases) for 4 of the considered

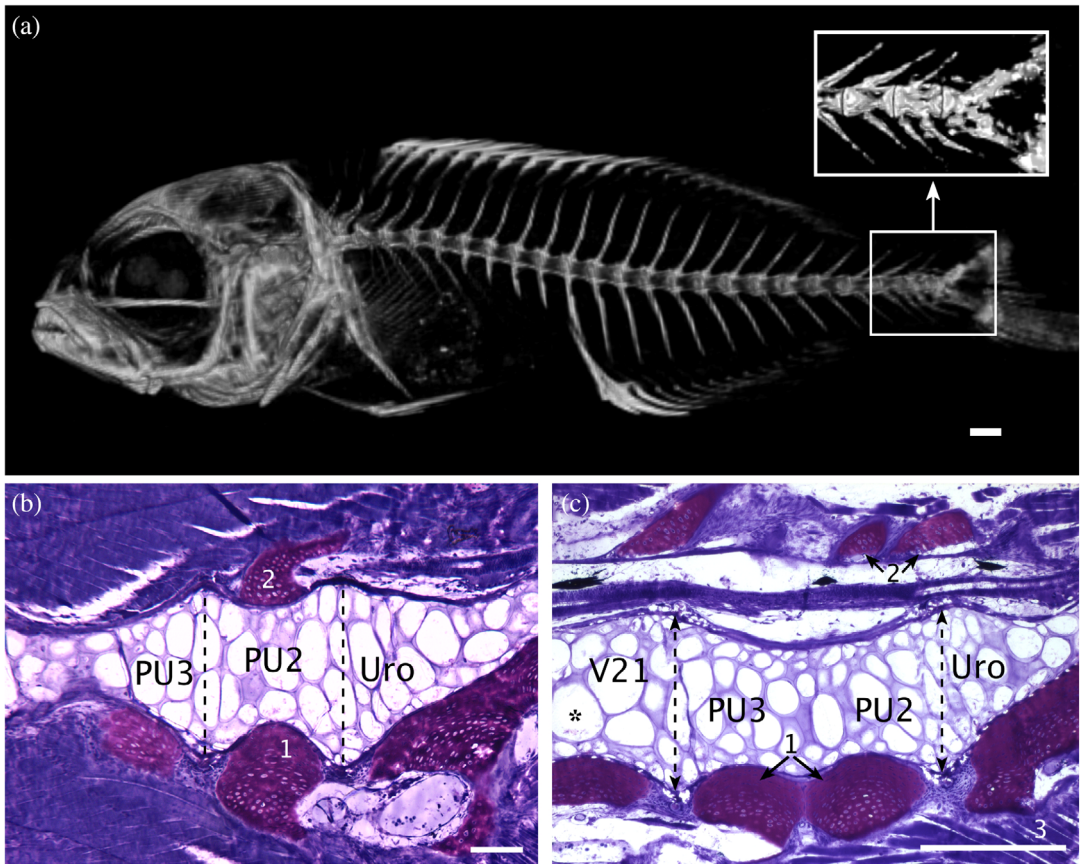


**FIGURE 11** (a) Micro-CT reconstruction of a gilthead seabream (lateral view, SL = 15.43 mm) showing a putative fusion of caudal vertebral bodies; (b) normally shaped caudal vertebral bodies of another specimen (SL = 12.98 mm); (c) sagittal sections of the vertebrae highlighted in the rectangular selection of the Micro-CT reconstruction. The histological evaluation confirms the presence of a fusion between the two preural vertebrae (PU3 and PU2); compared with (b). The modeling of the intervertebral ligament between the fusing centra is advanced dorsally. Ventrally, the two vertebral centra are still discernible. V21: last (terminal) hemal vertebra; PU3 and PU2 = preural vertebrae 3 and 2; Uro = urostyle; asterisk = notochord vacuole; 1 = Hyaline cartilage at the base of hemal arches; 2 = Hyaline cartilage of the neural arches; 3 = myomere. (b) and (c) Toluidine blue staining. Scale bar for MicroCT image = 0.5 mm. Scale bars for histological sections = 0.2 mm.

groups of anomalies (Tables 2–5). Interestingly, the category of the vertebral body shape anomalies not only discriminated between gilthead seabream reared at different densities (with the same water volumes) but also between those reared in different volumes at equivalent densities (LD1000 vs. LD500, MD1000 vs. MD500, HD1000 vs. HD500).

### 3.3.2 | Correspondence analysis

A preliminary CA was applied to the RM consisting of 949 individuals and 70 anomalies types. However, the ordination model displayed an extremely low variance for the respective axes. Therefore, other CAs were performed on different subsets of anomalies and the highest variance expressed by the first two correspondence axes (CA1: 35.85%;



**TABLE 2** Results of  $\chi^2$  pairwise post hoc of frequencies of juvenile gilthead seabream affected by vertebral body shape anomalies among the conditions.

	MD1000	HD1000	LD500	MD500	HD500
LD1000	****	****	****	****	****
MD1000		****	****	****	NS
HD1000			NS	NS	****
LD500				NS	****
MD500					****

Note: Significant ( $p < 0.05$ ) differences are highlighted by asterisks: \* $0.05 > p\text{-value} > 0.01$ ; \*\* $0.01 > p\text{-value} > 0.001$ ; \*\*\* $0.001 > p\text{-value} > 0.0001$ ; \*\*\*\* $p\text{-value} < 0.0001$ ; NS: not statistically significant.

**TABLE 3** Results of  $\chi^2$  pairwise post hoc of frequencies of juvenile gilthead seabream affected by arch anomalies (5\* and 6\*) among the conditions.

	MD1000	HD1000	LD500	MD500	HD500
LD1000	***	****	NS	**	**
MD1000		NS	**	NS	NS
HD1000			**	NS	NS
LD500				NS	*
MD500					NS

Note: Significant ( $p < 0.05$ ) differences are highlighted by asterisks: \* $0.05 > p\text{-value} > 0.01$ ; \*\* $0.01 > p\text{-value} > 0.001$ ; \*\*\* $0.001 > p\text{-value} > 0.0001$ ; \*\*\*\* $p\text{-value} < 0.0001$ ; NS: not statistically significant.

**TABLE 4** Results of  $\chi^2$  pairwise post hoc of frequencies of juvenile gilthead seabream affected by severe anomalies among the conditions.

	MD1000	HD1000	LD500	MD500	HD500
LD1000	*	****	NS	**	***
MD1000		*	NS	NS	NS
HD1000			*	NS	NS
LD500				NS	NS
MD500					NS

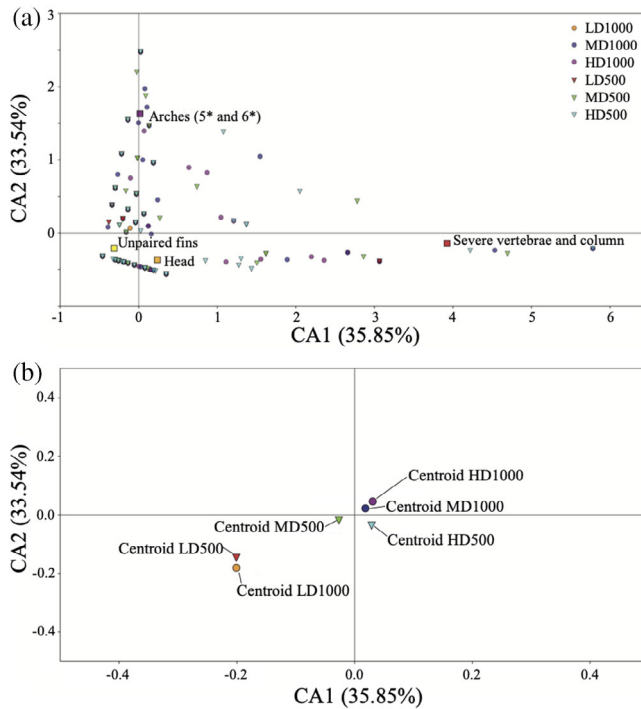
Note: Significant ( $p < 0.05$ ) differences are highlighted by asterisks: \* $0.05 > p\text{-value} > 0.01$ ; \*\* $0.01 > p\text{-value} > 0.001$ ; \*\*\* $0.001 > p\text{-value} > 0.0001$ ; \*\*\*\* $p\text{-value} < 0.0001$ ; NS: not statistically significant.

CA2: 33.54%) was obtained by applying the CA to an RM consisting of 860 individuals and four categories of anomalies. This matrix was built using 37 of the 70 observed anomalies that were grouped (as shown in Table S3) into four categories: severe anomalies of the vertebrae and column (that includes complete and partial vertebral fusions, hemi-vertebrae, and scoliosis), head anomalies (viz., jaws and opercular anomalies), anomalies of associated arches (super-numerary or absence of neural and/or hemal arches and spines), and anomalies affecting the unpaired fins (rays and pterygophores of the dorsal and anal fins and the rays, hypurals, and epurals of the caudal fin). Consequently, a total of 89 individuals without these anomalies had to be removed from the analysis because a null data vector (a specimen without any of the considered anomalies) cannot be analyzed with vector normalization methods such as those required for a CA. The resulting ordination model of all the individuals and descriptors (viz. the four anomaly categories) is shown in Figure 12a and the ordination of lot centroids in Figure 12b. Even though individuals are

**TABLE 5** Results of  $\chi^2$  pairwise post hoc of frequencies of juvenile gilthead seabream affected by jaw anomalies among the conditions.

	MD1000	HD1000	LD500	MD500	HD500
LD1000	*	**	NS	**	***
MD1000		NS	NS	NS	NS
HD1000			NS	NS	NS
LD500				NS	*
MD500					NS

Note: Significant ( $p < 0.05$ ) differences are highlighted by asterisks: \* $0.05 > p\text{-value} > 0.01$ ; \*\* $0.01 > p\text{-value} > 0.001$ ; \*\*\* $0.001 > p\text{-value} > 0.0001$ ; \*\*\*\* $p\text{-value} < 0.0001$ ; NS: not statistically significant.

**FIGURE 12** Results of Correspondence Analysis (CA) applied to the raw matrix of data inherent to 850 individuals and four anomaly categories. (a) ordination model of all individuals and descriptors (anomalies grouped as shown in Table S3); (b) ordination model of lot centroids. Note the increased magnification with respect to the graph shown in (a).

mostly concentrated (often overlapping) in the third quadrant (Figure 12a), the lot centroids are positioned in the first, third, and fourth quadrants (Figure 12b). Both the centroids of the low-density groups (LD1000 and LD500) are plotted on the third quadrant, relatively near to each other. MD500 is also located in the third but nearer to the axes' origin, as well as the category of anomalies affecting the unpaired fins (Figure 12a). In the opposite plane and quadrant, MD1000 and HD1000 centroids are located (quadrant 1, Figure 12b) and sharing quadrant 1 (although they are not proximal) with anomalies of vertebral arches (5\* and 6\*). The HD500 centroid is plotted in the fourth quadrant, sharing the quadrant proximally with head anomalies and distally with the severe vertebrae and column anomalies.

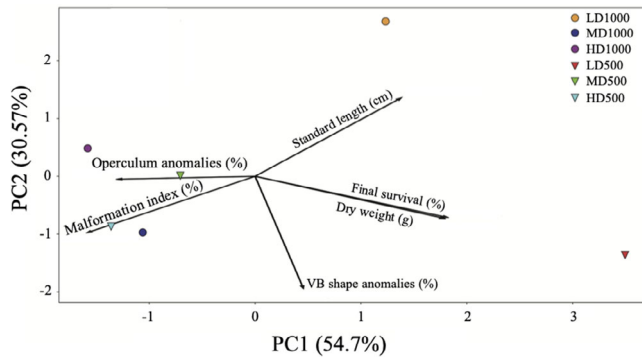


**FIGURE 13** PCA performed to recognize the association between experimental rearing conditions and some descriptors. The resulting ordination suggests that the low-density conditions are associated with favorable output features such as survival, weight, and length of the individuals while negatively related to skeletal anomalies.

### 3.3.3 | Principal component analysis

A PCA was performed to recognize general patterns associated with the rearing conditions. The following 6 variables were selected to perform the ordination: SL, survivorship, DW, vertebral body shape anomalies, malformation index, and opercular anomalies (Figure 13). Type one scaling was used since the principal focus was on the relative position of the conditions. By using this type of scaling, the distance between the objects in the plot approximates their Euclidean distances in full-dimensional space. The variance explained by the principal components 1 and 2 was 54.7% and 30.57%, respectively. The large share of variance explained by the first two axes highlights that the structure behind the data is relatively simple and justifies an unconventional use of the PCA, which usually requires a larger number of observations with respect to the considered variables. The ordination enables the observation of several key features based on the different rearing conditions. From a general perspective, a greater survival rate resulted to be closely associated with greater DW(g). On the other hand, the malformation index (viz. the average number of anomalies for each deformed gilthead seabream, per group), and the percentage of opercular anomalies indicate the opposite direction along the first component. Moreover, the ordination suggests the existence of a positive relationship between the length of the individuals and the low-density conditions while the malformation index and the opercular anomaly vectors represent a dominant influence in the high and medium-density conditions (Figure 13).

## 4 | DISCUSSION

This study was aimed at investigating if the same effects of rearing density already described on skeletal anomalies in two model species (medaka and zebrafish) and in gilthead seabream during the pre-ongrowing phase (from different egg-batches and parents) would be found in gilthead seabream juveniles reared from 0 up to 60 dph from the same egg-batch and broodstock. The tested densities were chosen based on the requests of the Italian Fish Farmers Association (API) while the experimental water volumes were equivalent to those tested in the pre-ongrowing experiment carried out on sub-adult gilthead seabream. As in the pre-ongrowing trial, the experimental conditions were tested at a pilot study (on a total of 615,385 eggs), without replicates. This choice was based on the consideration that the use of the tested densities in tanks with volumes greater than 1000 L or with replicas of such tanks would require an exceedingly high number of initial larvae that it would be impossible to obtain enough eggs from the same spawning event, reared throughout the entirety of larval ontogenesis during the same period, thereby potentially

introducing other variables to the experimental conditions. Furthermore, the final observations were carried out on a large number of individual fish to thoroughly classify the effects of the conditions on the entirety of the skeleton (>249/condition).

The densities tested in this trial (25 vs. 125 vs. 250 larvae/L) were much higher than those reported in previous density-related comparisons (3–16 larvae/L versus 100 larvae/L), while the compared volumes were smaller (500 and 1000 L) than those previously investigated (small volumes: 500 or 900 L versus mesocosms or large volumes: 40,000 or 60,000 L, respectively) (Prestinicola et al., 2013). Bearing in mind the objective to maintain only the rearing density and the water volume as the factors under examination, the other rearing conditions were maintained consistent among all the tanks during the experimental trial. Necessarily, the velocity rate of water flow differed between the 1000-L tanks and the 500-L tanks: in order to maintain the same water replacement rate, water had to be pumped in faster to replace 1000 L in the equivalent time as the 500-L tanks. Recent studies on gilthead seabream juveniles have found that increased water flow can induce an ‘exercise behavior’, resulting in an improved growth rate (Moya et al., 2019), muscle building, energy mobilization, robustness, and reduced stress, although lordotic juvenile gilthead seabream were found to be more frequent when fish were reared in tanks with higher flow rates (Palstra et al., 2020). In the present study, lordotic fish were not found, possibly as a result of the early juvenile stage of the final sampling (average SL = 1.79 cm). Additionally, the flow rates in this study were generally lower than flow rates used to provoke the exercise response, even during the end of rearing in the 1000-L tanks, in which water flow was increased up to 100%/h, and flow velocities were ~0.73 and ~0.36 m/s from the inlet for 1000-L and 500-L tanks, respectively. Taking into consideration that this velocity is not uniform throughout the tank, and that peak velocity was limited to the water inlet and differentially distributed between the borders and the center of the tank (Oca & Masalo, 2013), fish should have been able to swim in the zone of their preferred water flux.

#### 4.1 | General performances

The final survival rates obtained in this study at 60 dph (after weaning had been completed) ranged from 3.3% to 29.7%. Survival rates in gilthead seabream larvae reared in experimental conditions can vary greatly: for example, survival from 0–22 dph can range from 3% to 50% (Pousão-Ferreira et al., 2003) and from 20–44 dph can range from 7% to 23% (Izquierdo et al., 2017). The results from this work suggested that stocking density strongly affected final survival at 60 dph. Both LD tanks had higher survival rates, and the overall significantly highest survival obtained was found in the LD500 condition.

Early juveniles from the LD conditions produced the longest and heaviest juveniles overall, while the fish from the MD and HD conditions were the shortest and lightest. A secondary volume effect could be observed in both LD and HD conditions, where the tanks of 1000 L produced fish longer than the 500-L ones, at the same densities. Notably, the greater lengths of LD juveniles were not correlated to the number of vertebrae, whose range on the contrary included the lowest count.

A previous work on larval rearing of gilthead seabream reared using the pseudo-green water technique found similar final sizes to the LD gilthead seabream in this work. However, they achieved better final growth at 60 dph (TL: ~20 mm) (Papandroulakis et al., 2001) than the MD and HD conditions from this present study. This could have been a result of the fact that they used ~100 larvae/L in 500 L tanks up to ~30 dph and then transferred the fish to larger tanks (2m<sup>3</sup>) stocked at lower densities (~50 larvae/L). Other factors such as a late spawning season and colder seawater temperatures likely also played a role in the limited growth observed in this current study with respect to other published data.

The LD conditions facilitated higher survival, final weights, and lengths in reared gilthead seabream larvae after 60 days. This finding is corroborated by several recent findings. Similar findings have been observed in medaka (reared from 0 to 40 dph), displaying greater TL and proportionally augmented survival rates with lower rearing densities (Di Biagio et al., 2022). Similarly, in zebrafish (reared from 30 to 90 dph), the SL decreased with the increasing

rearing densities (Martini et al., 2021). Significantly greater TL, but not weight, was also found in the fish reared in low-density conditions (5 kg/m<sup>3</sup>) from a recent experiment on gilthead seabream subadults (Dellacqua et al., 2023). Another study rearing adult gilthead seabream (~271 g) for 9 weeks at three density conditions (5, 10, and 20 kg/m<sup>3</sup>) revealed the same inverse relationship between increasing density and fish size (both weights and length, in this latter case) (Araújo-Luna et al., 2018). Concerning salmonids, studies on 82 g rainbow trout (*Oncorhynchus mykiss*) (Zoccarato et al., 1994) and <2.4 g coho salmon (*O. kisutch*) (Fagerlund et al., 1981) reported negative effects on growth when the rearing densities were too high. Conversely, pre-ongrowing of ~6.6 g European seabass (*D. labrax*) (Papoutsoglou et al., 1998) and fattening of ~53.8 g arctic char (*Salvelinus alpinus*) (Jørgensen et al., 1993) showed improved growth rates at higher stocking densities rather than lower ones. These studies indicate some species-specific differences in response to varying densities.

## 4.2 | Skeletal anomalies

The results obtained from this study have evidenced that while a diversity of anomaly types may have been present without being influenced by the rearing density (considered as ‘background’ anomalies), the incidences of some less frequent anomalies (i.e., affecting jaws, vertebral body shape, and vertebral arches) were significantly reduced in lower densities (evidenced namely by the CA, PCA,  $\chi^2$  test, and  $\chi^2$  pairwise post hoc tests). The lowest malformation index and frequency of gilthead seabream with at least one severe anomaly resulted in being significantly associated with the LD conditions (Table 1). Concerning the effect of the stocking density, sub-adults of gilthead seabream (54.9 g), after having been reared at low density (5 kg/m<sup>3</sup>) for 63 days during the pre-ongrowing phase (starting from 6.7 g) showed significant reductions in frequencies of individuals affected by opercular plate anomalies, lordosis, and kyphosis (Dellacqua et al., 2023). Furthermore, lower densities have been found to reduce the incidences of skeletal anomalies in model fish species reared in laboratory settings (Di Biagio et al., 2022; Martini et al., 2021). Additionally, the water volumes seem to play a slight secondary effect on the skeleton during the hatchery phase of gilthead seabream, although only significantly different for the vertebral body shape anomalies.

Concerning anomalies of the head, opercular anomalies are quite important for farmers because they facilitate the infestation of parasites in the gills, and these anomalies are externally detectable on marketed fish. Although in the tested conditions from this study, opercular anomalies affected relatively few individuals, their frequencies displayed a direct relationship with both density and water volume, even though the differences were not significant. In a previous experiment carried out on pre-ongrowing juveniles (Dellacqua et al., 2023), it was found that gilthead seabream exhibiting opercular anomalies were significantly more frequent in sub-adults from the HD1000 condition compared to the LD conditions. The gilthead seabream from HD500 condition also exhibited an increased occurrence of individuals affected by opercular anomalies, although this was not significantly different. On the contrary, jaw anomalies in this current study displayed significantly augmented incidences in HD larvae (but with no significant effect of water volume), while in pre-ongrowing subadults the incidences of jaw anomalies augmented in HD conditions (and in lower water volumes), although not significantly. The discrepancy in the effects of water volume observed on opercular plates and jaws, which are both located in the splanchnocranium, share the same neural crest origin (Hall, 2015), and are formed around a cartilaginous precursor, confirms previous observations that the same environmental factor (i.e., water volume) may induce different incidences of anomalies affecting skeletal elements of the same bone type and ossification mode (Fernández & Gisbert, 2011), in the same species. This could be as a result of the different functionality (i.e., biting vs. ventilation) of the involved bones (i.e., maxillary/premaxillary and opercular plate) which were not equally acted on by varying stocking densities.

Interestingly, even the fusions and hemivertebrae in the caudal centra showed a significantly augmented prevalence with increased density. The caudal fin enables controlled quick movements in the water column and is a key component in predatory escape responses (Gibb et al., 2006). Furthermore, caudal fin development represents a critical stage in rousing key behavioral changes in the early ontogeny of fishes (Somarakis & Nikolioudakis, 2010). As a result of the particular nature of this region, some environmental factors such as water flow rate, space availability

and utilization, stocking density, and type/quantity of individual interactions may yield different swimming behaviors that cause different interactions between muscles and bone. Nevertheless, caudal region sensitivity to skeletal anomalies has been previously proposed to be a species-specific characteristic of gilthead seabream (Koumoundouros et al., 1997), as even some (rare) wild gilthead seabream have been found with anomalies in this region (Boglione et al., 2001).

## 5 | CONCLUSIONS

The hatchery rearing of marine fish, such as gilthead seabream, represents a particularly sensitive phase of development in which many different etiological factors, often acting synergistically, determine the incidences of fish with skeletal anomalies. This investigation aimed to verify if the same effects of only two pivotal factors, density and water volume, on the skeletal phenotype described in two model species and in a different rearing (and life) phase in gilthead seabream were identifiable from juveniles produced during the hatchery (larval) phase. The obtained results confirm that high stocking density, rather than the available water volume, seems to facilitate significantly greater frequencies of skeletal anomalies of the jaws, vertebral bodies, and arches in gilthead seabream post-larvae. Behavioral or metabolic factors may have also been involved in the modeling processes leading to the higher rates of anomalies found in fish from the high-density conditions, at least in this experimental trial, for this species, and at this life stage. Future research should include anatomical, histological, and statistical analyses, as well as biochemical, behavioral, and epigenetic data from additional replicates.

## ACKNOWLEDGMENTS

We would like to thank the team at ULPGC for their support, especially Carmen Maria Hernandez-Cruz and Daniel Montero for their support in setting up the experimental protocols. We would also like to thank David Dominguez and Shajahan Ferosekhan for their assistance in the experimental setup as well as Yiyen Tseng and Sivagurunathan Ulaganthan for their help in sampling. We would also like to thank the technicians at ECOAQUA for their constant support in rearing and troubleshooting. Additionally, we would like to thank Eckhard Witten from the University of Ghent for his help in histological interpretation.

## FUNDING INFORMATION

This research was funded by European Union's Horizon 2020 research and innovation program 'BIOMEDAQU' under the Marie Skłodowska-Curie grant agreement No.766347.

## DATA AVAILABILITY STATEMENT

The data that support the findings of this study are available from the corresponding author upon reasonable request.

## ORCID

Zachary Dellacqua  <https://orcid.org/0009-0001-5052-4350>

Arianna Martini  <https://orcid.org/0000-0001-5283-7521>

## REFERENCES

- Afonso, J. M., Montero, D., Robaina, L., Astorga, N., Izquierdo, M. S., & Gines, R. (2000). Association of a lordosis-scoliosis-kyphosis deformity in gilthead seabream (*Sparus aurata*) with family structure. *Fish Physiology and Biochemistry*, 22, 159–163. <https://doi.org/10.1023/A:1007811702624>
- Araújo-Luna, R., Ribeiro, L., Bergheim, A., & Pousão-Ferreira, P. (2018). The impact of different rearing condition on gilthead seabream welfare: Dissolved oxygen levels and stocking densities. *Aquaculture Research*, 49(12), 3845–3855. <https://doi.org/10.1111/are.13851>

- Baeverfjord, G., Antony Jesu Prabhu, P., Fjelldal, P. G., Albrektsen, S., Hatlen, B., Denstadli, V., Ytteborg, E., Takle, H., Lock, E. J., Bernstssen M. H. G., Lundebye, A. K., Åsgård, T., & Waagbø, R. (2019). Mineral nutrition and bone health in salmonids. *Reviews in Aquaculture*, 11(3), 740–765. <https://doi.org/10.1111/raq.12255>
- Benjamini, Y., & Hochberg, Y. (1995). Controlling the false discovery rate: A practical and powerful approach to multiple testing. *Journal of the Royal Statistical Society: Series B (Methodological)*, 57(1), 289–300. <https://doi.org/10.1111/j.2517-6161.1995.tb02031.x>
- Benzecri, J. P. (1975). L'Analyse des Donne'es. L'Analyse des Correspondances, vol. 2. Dunod, Paris, France. p. 628.
- Berillis, P. (2017). Skeletal deformities in seabreams. Understanding the genetic origin can improve production? *Journal of Fisheries Sciences.Com*, 11(2), 57. <https://doi.org/10.21767/1307-234x.1000118>
- Boglione, C., Gagliardi, F., Scardi, M., & Cataudella, S. (2001). Skeletal descriptors and quality assessment in larvae and post-larvae of wild-caught and hatchery-reared gilthead sea bream (*Sparus aurata* L. 1758). *Aquaculture*, 192(1), 1–22. [https://doi.org/10.1016/S0044-8486\(00\)00446-4](https://doi.org/10.1016/S0044-8486(00)00446-4)
- Boglione, C., Gavaia, P., Koumoundouros, G., Gisbert, E., Moren, M., Fontagné, S., & Witten, P. E. (2013). Skeletal anomalies in reared E uropean fish larvae and juveniles. Part 1: Normal and anomalous skeletogenic processes. *Reviews in Aquaculture*, 5, S99–S120. <https://doi.org/10.1111/raq.12015>
- Boglione, C., Gisbert, E., Gavaia, P. E., Witten, P., Moren, M., Fontagné, S., & Koumoundouros, G. (2013). Skeletal anomalies in reared E uropean fish larvae and juveniles. Part 2: Main typologies, occurrences and causative factors. *Reviews in Aquaculture*, 5, S121–S167. <https://doi.org/10.1111/raq.12016>
- Boglione, C., Marino, G., Giganti, M., Longobardi, A., De Marzi, P., & Cataudella, S. (2009). Skeletal anomalies in dusky grouper *Epinephelus marginatus* (Lowe 1834) juveniles reared with different methodologies and larval densities. *Aquaculture*, 291(1–2), 48–60. <https://doi.org/10.1016/j.aquaculture.2009.02.041>
- Cahu, C., Infante, J. Z., & Takeuchi, T. (2003). Nutritional components affecting skeletal development in fish larvae. *Aquaculture*, 227(1–4), 245–258. [https://doi.org/10.1016/S0044-8486\(03\)00507-6](https://doi.org/10.1016/S0044-8486(03)00507-6)
- Cataudella, S., Russo, T., Cataldi, E., Boglione, C., & Saroglia, M. (2003). Does the model of semi-intensive larval rearing of Mediterranean finfish contribute to the knowledge on animal welfare in aquaculture? In Proceedings of the International Aquaculture Conference, Fish Farming in Mediterranean Europe: Quality for Developing Markets, Verona, Italy, October 2003; Geatti, F., Berardo, P. & Zanchetta, S., eds; Book of Abstracts: 49.
- Chatain, B., & Ounais-Guschemann, N. (1990). Improved rate of initial swim bladder inflation in intensively reared *Sparus aurata*. *Aquaculture*, 84(3–4), 345–353. [https://doi.org/10.1016/0044-8486\(90\)90099-9](https://doi.org/10.1016/0044-8486(90)90099-9)
- Darias, M. J., Mazurais, D., Koumoundouros, G., Cahu, C. L., & Zambonino-Infante, J. L. (2011). Overview of vitamin D and C requirements in fish and their influence on the skeletal system. *Aquaculture*, 315(1–2), 49–60. <https://doi.org/10.1016/j.aquaculture.2010.12.030>
- Dellacqua, Z., Di Biagio, C., Costa, C., Pousão-Ferreira, P., Ribeiro, L., Barata, M., Gavaia, P., Mattei, F., Fabris, A., Izquierdo, M., & Boglione, C. (2023). Distinguishing the effects of water volumes versus stocking densities on the skeletal quality during the pre-Ongrowing phase of gilthead seabream (*Sparus aurata*). *Animals*, 13(4), 557. <https://doi.org/10.3390/ani13040557>
- Di Biagio, C. (2022). Unveiling Skeletal Phenotypes of Fish Models in Response to Environmental Factors: A Multi-disciplinary Approach. Ph.D. thesis, University of Rome 'Tor Vergata' and Ghent University, Rome, Italy, December.
- Di Biagio, C., Dellacqua, Z., Martini, A., Huysseune, A., Scardi, M., Witten, P. E., & Boglione, C. (2022). A baseline for skeletal investigations in Medaka (*Oryzias latipes*): The effects of rearing density on the postcranial phenotype. *Frontiers in Endocrinology*, 13, 893699. <https://doi.org/10.3389/fendo.2022.893699>
- Divanach, P., & Kentouri, M. (2000). Hatchery techniques for specific diversification in Mediterranean finfish larviculture. *Cahiers Options Mediterraneeennes*, 47, 75–87.
- Dominguez, D., Castro, P., Lall, S., Montero, D., Zamorano, M. J., Fontanillas, R., & Izquierdo, M. (2022). Effects of Menadione sodium Bisulphite (vitamin K3) supplementation of the diets based on plant feed ingredients on growth and bone health of gilthead seabream (*Sparus aurata*) fingerlings. *Aquaculture Nutrition*, 2022, 1–8. <https://doi.org/10.1155/2022/1613030>
- Dominguez, D., Montero, D., Zamorano, M. J., Castro, P., Fontanillas, R., Prabhu, P. A. J., & Izquierdo, M. (2021). Effects of vitamin D3 supplementation in gilthead seabream (*Sparus aurata*) juveniles fed diets high in plant based feedstuffs. *Aquaculture*, 543, 736991. <https://doi.org/10.1016/j.aquaculture.2021.736991>
- Eissa, A. E., Abu-Seida, A. M., Ismail, M. M., Abu-Elala, N. M., & Abdelsalam, M. (2021). A comprehensive overview of the most common skeletal deformities in fish. *Aquaculture Research*, 52(6), 2391–2402. <https://doi.org/10.1111/are.15125>
- European Parliament. (2018). Fact sheets on the European Union: European fisheries in figures. <https://www.europarl.europa.eu/factsheets/en/sheet/122/european-fisheries-in-figures>
- Fagerlund, U. H. M., McBride, J. R., & Stone, E. T. (1981). Stress-related effects of hatchery rearing density on coho salmon. *Transactions of the American Fisheries Society*, 110(5), 644–649. [https://doi.org/10.1577/1548-8659\(1981\)110<644:SEOHRD>2.0.CO;2](https://doi.org/10.1577/1548-8659(1981)110<644:SEOHRD>2.0.CO;2)



- Faustino, M., & Power, D. M. (1998). Development of osteological structures in the sea bream: Vertebral column and caudal fin complex. *Journal of Fish Biology*, 52(1), 11–22. <https://doi.org/10.1111/j.1095-8649.1998.tb01548.x>
- Fernández, I., & Gisbert, E. (2011). The effect of vitamin a on flatfish development and skeletogenesis: A review. *Aquaculture*, 315(1–2), 34–48. <https://doi.org/10.1016/j.aquaculture.2010.11.025>
- Ferosekhan, S., Sarih, S., Afonso, J. M., Zamorano, M. J., Fontanillas, R., Izquierdo, M., Kaushik, S., & Montero, D. (2022). Selection for high growth improves reproductive performance of gilthead seabream *Sparus aurata* under mass spawning conditions, regardless of the dietary lipid source. *Animal Reproduction Science*, 241, 106989. <https://doi.org/10.1016/j.anireprosci.2022.106989>
- Ferosekhan, S., Xu, H., Turkmen, S., Gómez, A., Afonso, J. M., Fontanillas, R., Rosenlund, G., Kaushik, S., & Izquierdo, M. (2020). Reproductive performance of gilthead seabream (*Sparus aurata*) broodstock showing different expression of fatty acyl desaturase 2 and fed two dietary fatty acid profiles. *Scientific Reports*, 10(1), 1–14. <https://doi.org/10.1038/s41598-020-72166-5>
- Fragkouli, S., Batargias, C., Kolios, P., & Koumoundouros, G. (2018). Genetic parameters of the upper-jaw abnormalities in gilthead seabream *Sparus aurata*. *Aquaculture*, 497, 226–233. <https://doi.org/10.1016/j.aquaculture.2018.07.071>
- Fragkouli, S., Economou, I., Moukas, G., Koumoundouros, G., & Batargias, C. (2020). Caudal fin abnormalities in gilthead seabream (*Sparus aurata* L.) have a strong genetic variance component. *Journal of Fish Diseases*, 43(7), 825–828. <https://doi.org/10.1111/jfd.13180>
- Fragkouli, S., Printzi, A., Geladakis, G., Katribouzas, N., & Koumoundouros, G. (2019). Recovery of haemal lordosis in gilthead seabream (*Sparus aurata* L.). *Scientific Reports*, 9(1), 1–11. <https://doi.org/10.1038/s41598-019-46334-1>
- Georga, I., Glyntsi, N., Baltzois, A., Karamanos, D., Mazurais, D., Darias, M. J., Cahu C. L., Zambonino-Infante, J. L., & Koumoundouros, G. (2011). Effect of vitamin a on the skeletal morphogenesis of European sea bass, *Dicentrarchus labrax* (Linnaeus, 1758). *Aquaculture Research*, 42(5), 684–692. <https://doi.org/10.1111/j.1365-2109.2010.02676.x>
- Gibb, A. C., Swanson, B. O., Wesp, H., Landels, C., & Liu, C. (2006). Development of the escape response in teleost fishes: Do ontogenetic changes enable improved performance? *Physiological and Biochemical Zoology*, 79(1), 7–19. <https://doi.org/10.1086/498192>
- Hall, B. K. (2015). *Bones and cartilage: Developmental and evolutionary skeletal biology*. Elsevier Ltd.
- Hamre, K., Yufera, M., Rønnestad, I., Boglione, C., Conceição, L. E., & Izquierdo, M. (2013). Fish larval nutrition and feed formulation: Knowledge gaps and bottlenecks for advances in larval rearing. *Reviews in Aquaculture*, 5, S26–S58. <https://doi.org/10.1111/j.1753-5131.2012.01086.x>
- Izquierdo, M., Domínguez, D., Jiménez, J. I., Saleh, R., Hernández-Cruz, C. M., Zamorano, M. J., & Hamre, K. (2019). Interaction between taurine, vitamin E and vitamin C in microdiets for gilthead seabream (*Sparus aurata*) larvae. *Aquaculture*, 498, 246–253. <https://doi.org/10.1016/j.aquaculture.2018.07.010>
- Izquierdo, M., Ghrab, W., Roo, J., Hamre, K., Hernández-Cruz, C. M., Bernardini, G., Terova, G., & Saleh, R. (2017). Organic, inorganic and nanoparticles of Se, Zn and Mn in early weaning diets for gilthead seabream (*Sparus aurata*; Linnaeus, 1758). *Aquaculture Research*, 48(6), 2852–2867. <https://doi.org/10.1111/are.13119>
- Jørgensen, E. H., Christiansen, J. S., & Jobling, M. (1993). Effects of stocking density on food intake, growth performance and oxygen consumption in Arctic charr (*Salvelinus alpinus*). *Aquaculture*, 110(2), 191–204. [https://doi.org/10.1016/0044-8486\(93\)90272-Z](https://doi.org/10.1016/0044-8486(93)90272-Z)
- Koumoundouros, G., Gagliardi, F., Divanach, P., Boglione, C., Cataudella, S., & Kentouri, M. (1997). Normal and abnormal osteological development of caudal fin in *Sparus aurata* L. fry. *Aquaculture*, 149(3–4), 215–226. [https://doi.org/10.1016/s0044-8486\(96\)01443-3](https://doi.org/10.1016/s0044-8486(96)01443-3)
- Kourkouta, C., Tsiourlianos, A., Power, D. M., Moutou, K. A., & Koumoundouros, G. (2022). Variability of key-performance-indicators in commercial gilthead seabream hatcheries. *Scientific Reports*, 12(1), 17896. <https://doi.org/10.1038/s41598-022-23008-z>
- Lall, S. P., & Lewis-McCrea, L. M. (2007). Role of nutrients in skeletal metabolism and pathology in fish—An overview. *Aquaculture*, 267(1–4), 3–19. <https://doi.org/10.1016/j.aquaculture.2007.02.053>
- Llorente, I., Fernández-Polanco, J., Baraibar-Díez, E., Odriozola, M. D., Bjørndal, T., Asche, F., Guillen, J., Avdelas, L., Nielsen, R., Cozzolino, M., Luna, M., Fernández-Sánchez, J. L., Luna, L., Aguilera, C., & Basurco, B. (2020). Assessment of the economic performance of the seabream and seabass aquaculture industry in the European Union. *Marine Policy*, 117, 103876. <https://doi.org/10.1016/j.marpol.2020.103876>
- Martini, A., Huysseune, A., Witten, P. E., & Boglione, C. (2021). Plasticity of the skeleton and skeletal deformities in zebrafish (*Danio rerio*) linked to rearing density. *Journal of Fish Biology*, 98(4), 971–986. <https://doi.org/10.1111/jfb.14272>
- Moya, A., Torrella, J. R., Fernández-Borràs, J., Rizo-Roca, D., Millán-Cubillo, A., Vélez, E. J., Arcas, A., Gutiérrez, J., & Blasco, J. (2019). Sustained swimming enhances white muscle capillarisation and growth by hyperplasia in gilthead sea bream (*Sparus aurata*) fingerlings. *Aquaculture*, 501, 397–403. <https://doi.org/10.1016/j.aquaculture.2018.10.062>
- Oca, J., & Masalo, I. (2013). Flow pattern in aquaculture circular tanks: Influence of flow rate, water depth, and water inlet & outlet features. *Aquacultural Engineering*, 52, 65–72. <https://doi.org/10.1016/j.aquaeng.2012.09.002>

- Palstra, A. P., Roque, A., Kruijt, L., Jéhannet, P., Pérez-Sánchez, J., & Dirks, R. P. (2020). Physiological effects of water flow induced swimming exercise in seabream *Sparus aurata*. *Frontiers in Physiology*, 11, 610049. <https://doi.org/10.3389/fphys.2020.610049>
- Papandroulakis, N., Divanach, P., Anastasiadis, P., & Kentouri, M. (2001). The pseudo-green water technique for intensive rearing of sea bream (*Sparus aurata*) larvae. *Aquaculture International*, 9, 205–216. <https://doi.org/10.1023/A:1016813623122>
- Papoutsoglou, S. E., Tziha, G., Vrettos, X., & Athanasiou, A. (1998). Effects of stocking density on behavior and growth rate of European sea bass (*Dicentrarchus labrax*) juveniles reared in a closed circulated system. *Aquacultural Engineering*, 18(2), 135–144. [https://doi.org/10.1016/S0144-8609\(98\)00027-2](https://doi.org/10.1016/S0144-8609(98)00027-2)
- Pearson, K. (1900). X. On the criterion that a given system of deviations from the probable in the case of a correlated system of variables is such that it can be reasonably supposed to have arisen from random sampling. *The London, Edinburgh, and Dublin Philosophical Magazine and Journal of Science*, 50(302), 157–175. <https://doi.org/10.1080/14786440009463897>
- Pousão-Ferreira, P., Santos, P., Carvalho, A. P., Morais, S., & Narciso, L. (2003). Effect of an experimental microparticulate diet on the growth, survival and fatty acid profile of gilthead seabream (*Sparus aurata* L.) larvae. *Aquaculture International*, 11, 491–504. <https://doi.org/10.1023/B:AQU1.0000004190.13871.f3>
- Prestinicola, L., Boglione, C., Makridis, P., Spanò, A., Rimatori, V., Palamara, E., Scardi, M., & Cataudella, S. (2013). Environmental conditioning of skeletal anomalies typology and frequency in gilthead seabream (*Sparus aurata* L., 1758) juveniles. *PLoS One*, 8(2), e55736. <https://doi.org/10.1371/journal.pone.0055736>
- Sivagurunathan, U., Dominguez, D., Tseng, Y., Eryalçın, K. M., Roo, J., Boglione, C., Prabhu, A. J., & Izquierdo, M. (2022). Effects of dietary vitamin D3 levels on survival, mineralization, and skeletal development of gilthead seabream (*Sparus aurata*) larvae. *Aquaculture*, 560, 738505. <https://doi.org/10.1016/j.aquaculture.2022.738505>
- Somarakis, S., & Nikolioudakis, N. (2010). What makes a late anchovy larva? The development of the caudal fin seen as a milestone in fish ontogeny. *Journal of Plankton Research*, 32(3), 317–326. <https://doi.org/10.1093/plankt/fbp132>
- Taylor, W. R., & Van Dyke, G. C. (1985). Revised procedures for staining and clearing small fishes and other vertebrates for bone and cartilage study. *Cybio*, 9, 107–121. <https://ci.nii.ac.jp/naid/10013369229/>
- Tseng, Y., Dominguez, D., Bravo, J., Acosta, F., Robaina, L., Geraert, P. A., Kaushik, S., & Izquierdo, M. (2021). Organic selenium (OH-MetSe) effect on whole body fatty acids and mx gene expression against viral infection in gilthead seabream (*Sparus aurata*) juveniles. *Animals*, 11(10), 2877. <https://doi.org/10.3390/ani11102877>
- Van Rossum, G., & Drake, F. L., Jr. (1995). Python reference manual. Centrum voor Wiskunde en Informatica Amsterdam. <https://www.python.org/downloads/>.
- Witten, P. E., Hansen, A., & Hall, B. K. (2001). Features of mono-and multinucleated bone resorbing cells of the zebrafish *Danio rerio* and their contribution to skeletal development, remodeling, and growth. *Journal of Morphology*, 250(3), 197–207. <https://doi.org/10.1002/jmor.1065>
- Witten, P. E., Obach, A., Huyseune, A., & Baeverfjord, G. (2006). Vertebrae fusion in Atlantic salmon (*Salmo salar*): Development, aggravation and pathways of containment. *Aquaculture*, 258(1–4), 164–172. <https://doi.org/10.1016/j.aquaculture.2006.05.005>
- Zoccarato, I., Benatti, G., Bianchini, M. L., Boccignone, M., Conti, A., Napolitano, R., & Palmegiano, G. B. (1994). Differences in performance, flesh composition and water output quality in relation to density and feeding levels in rainbow trout, *Oncorhynchus mykiss* (Walbaum), farming. *Aquaculture Research*, 25(6), 639–647. <https://doi.org/10.1111/j.1365-2109.1994.tb00728.x>

## SUPPORTING INFORMATION

Additional supporting information can be found online in the Supporting Information section at the end of this article.

**How to cite this article:** Dellacqua, Z., Di Biagio, C., Martini, A., Mattei, F., Rakaj, A., Williams, J. C. Jr., Fabris, A., Izquierdo, M., & Boglione, C. (2024). Skeletal anomalies in gilthead seabream (*Sparus aurata*) larvae reared in different densities and water volumes. *Journal of the World Aquaculture Society*, e13056. <https://doi.org/10.1111/jwas.13056>